

Research Paper

Combined Use of Magnetization Transfer Ratio and T2-Mapping to Evaluate Extraocular Muscle Pathophysiology in Myasthenia Gravis with Ophthalmoparesis

Qin Zhou¹, Xiaoxiao Zhao¹, Mengzhu Wang², Yingkai Li^{3,4}, Zhiyun Yang¹, Weibin Liu^{4,5,6}, Pei Chen^{4,5,6}✉

1. Department of Radiology, The First Affiliated Hospital, Sun Yat-sen University, Guangzhou, China.
2. MR Scientific Marketing, Siemens Healthineers Ltd. Guangzhou, China.
3. Neuromuscular Division, Department of Neurology, Duke University Medical Center, Durham, United States.
4. Department of Neurology, The First Affiliated Hospital, Sun Yat-sen University, Guangzhou, China.
5. Guangdong Provincial Key Laboratory of Diagnosis and Treatment of Major Neurological Diseases, Guangzhou, China.
6. National Key Clinical Department and Key Discipline of Neurology, Guangzhou, China.

Qin Zhou and Xiaoxiao Zhao equally contributed to this study.

✉ Corresponding authors: Weibin Liu and Pei Chen; Weibin Liu; Email: liuwb@mail.sysu.edu.cn, ORCID: 0000-0003-1909-4898; Pei Chen, Email: chenp258@mail.sysu.edu.cn, ORCID: 0000-0002-3225-692X.

© The author(s). This is an open access article distributed under the terms of the Creative Commons Attribution License (<https://creativecommons.org/licenses/by/4.0/>). See <https://ivyspring.com/terms> for full terms and conditions.

Received: 2024.10.01; Accepted: 2024.10.19; Published: 2024.10.28

Abstract

Background Myasthenia gravis (MG) is an autoimmune neuromuscular disorder that most frequently affects the extraocular muscles (EOMs), which causes symptoms such as ptosis and restricted eye movement. The EOMs in MG patients are representative of autoimmune inflammatory changes in muscle tissue. Currently, there is no reliable, and sensitive imaging technique for monitoring EOM changes to assist in the evaluation of underlying pathological changes.

Methods This study included MG patients treated between March and November 2022 at the First Affiliated Hospital of Sun Yat-sen University. Healthy controls (matched by age and sex) were included. Participants underwent 3.0 T MRI with magnetization transfer imaging (MTI) and T2-mapping to measure the magnetization transfer ratio (MTR) and T2-mapping values in the superior, inferior, medial, and lateral rectus muscles. Comparisons were made between MG patients and healthy controls, and between MG subgroups with and without ophthalmoparesis.

Results The MTR and T2-mapping values successfully reflected EOM fibrosis and inflammatory edema in MG patients. MG patients showed significantly higher MTR and T2-mapping values in the EOMs compared with healthy controls. MG patients with ophthalmoparesis exhibited a lower MTR but higher T2-mapping value compared with those without ophthalmoparesis. Combined MTR and T2-mapping values effectively distinguished between MG patients and healthy controls, and between different severities of EOM involvement, with a superior diagnostic accuracy compared with each parameter alone.

Conclusion The combination of MTI and T2-mapping MRI techniques can provide key insight into the pathological changes in EOMs in MG patients. This approach enhances early diagnosis and treatment planning, and therefore may improve clinical outcomes.

Keywords: Myasthenia gravis, extraocular muscle, magnetization transfer imaging, T2-mapping, magnetization transfer ratio, ophthalmoparesis

Background

Myasthenia gravis (MG) is a typical neuro-immunological disorder caused by autoantibodies, which disrupt neurotransmitter signaling at the

neuromuscular junction and cause abnormal skeletal muscle fatigue [1, 2]. The extraocular muscles are the most affected skeletal muscles [3]. Although most MG

patients do not exhibit symptoms, persistent eyelid drooping and fixed or significantly restricted eye movement are frequently observed clinically, which can severely impact upon patients' daily life and appearance. MG patients often have a long medical history, and their extraocular muscles are significantly atrophied (suggestive of severe inflammation), particularly early in the disease course, which affects their function [4, 5]. Currently, there are limited techniques to quantitatively assess the extent of extraocular muscle involvement in MG patients in the early stages, and it is only possible to judge the extent of involvement based on the degree of eye movement limitation at that time [6, 7]. Furthermore, the extraocular muscle symptoms have received minimal clinical attention, which has limited the development of effective treatment strategies.

T2 mapping (i.e., the T2 relaxation time map) is a quantitative analysis technique that can measure the T2 value of tissues, and reflects changes in the extracellular fluid and collagen content [8]. T2 mapping is commonly used as a quantitative measure of water content in muscle tissue for assessment of inflammatory edema [9]. This MRI sequence is also often applied for clinical assessment of a range of diseases including Graves' ophthalmopathy (GO) [10]. Magnetization transfer imaging (MTI) primarily describes the physical process of magnetization transfer between free hydrogen nuclei and those bound to macromolecules in tissues, and indirectly reflects the concentration of macromolecules [11-13]. MTI has been recently used to assess the degree of pancreatic fibrosis before surgery [14], differentiate between fibrotic and inflammatory bowel strictures in Crohn's disease [15], and evaluate fibrosis following radiotherapy for rectal cancer [16], among other conditions [17-19].

To date, no studies have used MTI and T2 imaging to assess the inflammatory state of the extraocular muscles in MG patients. In the present study, we used MTI and T2 mapping sequences to evaluate the extraocular muscles of MG patients for assessment of pathophysiological changes in the extraocular muscles, and we provide important information for clinical diagnosis and treatment.

Materials and Methods

Subjects

This was a prospective study of patients who were clinically diagnosed with MG at the First Affiliated Hospital of Sun Yat-sen University from March 2022 to November 2022. Inclusion criteria were (1) confirmed MG and (2) completed orbital MRI examinations that included coronal MTI and

T2-mapping sequences. Exclusion criteria were (1) poor quality MRI images that did not meet the requirements for subsequent analysis, (2) concomitant hyperthyroidism, or (3) presence of other orbital or extraocular muscle disorders. Healthy controls were selected from another clinical study and underwent orbital MRI that included coronal MTI and T2-mapping sequences. The healthy controls included in the present study were matched by age and sex. Ethics approval for this study was obtained from the research ethics committee of the First Affiliated Hospital of Sun Yat-sen University (No. 2022-666). Informed consent was obtained from all participants. The authors affirm that human research participants provided informed consent to publish the images.

MG patient subgroup definitions

MG patients were classified into the MG-O (with ophthalmoparesis) and MG-N (without ophthalmoparesis) groups. Ophthalmoparesis was defined as a limitation of eye movement in any direction at the time of the study, without consideration of ptosis [20].

MRI protocol

All subjects underwent MRI in a 3.0-T scanner (Magnetom PRISMA; Siemens Healthineers, Erlangen, Germany) with a 64-channel transmit-receive head-coil (INVIVO, Gainesville, FL, USA). Patients were instructed to lie supine and close their eyes to reduce eye movement. The MTI was performed using two coronal three-dimensional gradient echo sequences with or without an off-resonance pre-pulse [21]. The scanning parameters were: repetition time = 34 ms, echo time = 6 ms, field of view = 220×165 mm², matrix = 256×256, bandwidth = 160 Hz/Px, 16 slices, slice thickness = 3 mm, voxel size = 0.9×0.9×3.0 mm³, flip angle = 10°, and acquisition time = 1:43 min. T2-mapping data were obtained using a T2 multi-spin-echo sequence. The acquisition parameters of the T2 sequences as following: repetition time=2000 ms, echo time=13.8, 27.6, 41.4, 55.2, 69.0ms, matrix 384×384, flip angle = 180°, bandwidth = 228 Hz/Px, 18 slices, slice thickness 3.0 mm and acquisition time = 4:54 min [13].

Image analysis

The magnetization transfer ratio (MTR) images were generated using Matlab code (R2021a, Mathworks, MA, USA). The T2-mapping values were carried out using syngo.via (VB20A_HF91) at Siemens workstation (Siemens Healthineers, Erlangen, Germany). MTR was calculated as $MTR = 1 - (MT1/MT0)$ [22], where MT0 is the local signal intensity of the gradient echo sequence without the

magnetization transfer saturation pulse, and MT1 is the local signal intensity of the gradient echo sequence with the magnetization transfer saturation pulse. On the MT-off images and T2 anatomical mapping images, a roughly circular region of interest (ROI) was manually drawn on the largest coronal section of the superior, medial, inferior, and lateral rectus muscles. Then the ROI were copy to the MTR image and T2-mapping image (Figure 1). The MTR and T2-mapping values for the left and right eyes were measured and recorded separately. Finally, the mean of MTR and T2-mapping values of the bilateral four rectus muscles (total eight rectus muscles) were used for statistical analysis. The quantitative parameters were measured by two neuroradiologists with more than seven years of experience in head and neck imaging diagnosis, who were blinded to the clinical data. The second radiologist reperformed the measurements after 1 month to assess inter-observer and intra-observer consistency. The first measurement by the second radiologist was used for the final statistical analysis.

Statistical analysis

Statistical analyses were performed using statistical software (SPSS v23.0, IBM Corp., Armonk, NY, USA; Prism v9.0, GraphPad software, Boston, MA, USA). The Kolmogorov–Smirnov test was used to assess the normality of quantitative data. Data following a normal distribution are expressed as mean±standard deviation (SD), and independent sample t-tests were used to compare the MTR and T2-mapping values between the two groups. Non-normally distributed data are expressed as

median (Q1, Q3), and the Mann-Whitney U test was used to compare age between the two groups. Fisher's test was used to compare differences in categorical data between groups. A binary logistic regression model was used to combine the MTR and T2-mapping values. Receiver operating characteristic (ROC) curves were used to evaluate the predictive ability of the MRI quantitative parameters MTR, T2-mapping values, and their combination for extraocular muscle inflammation or fibrosis, while the DeLong method was used to compare the area under the curve (AUC) [23]. A *p*-value <0.05 was considered statistically significant.

Results

Clinical data of enrolled patients

We enrolled 32 MG patients and 22 gender- and age-matched healthy controls (see Table 1 for age and gender data). The detailed clinical information of the enrolled patients and comparisons between the different MG subgroups are shown in Table 2.

Table 1. Comparison of the mean magnetization transfer ratio (MTR) and T2-mapping values between myasthenia gravis (MG) patients and healthy controls

	Ctrl (n=22)	MG (n=32)	T or Z value	P value
Age, years, mean±SD	43.91±22.04 (15-79)	44.97±18.11 (16-77)	0.1933	0.8474
Sex (male:female)	4:18	8:24		0.7416*
MTR, mean±SD	0.3147±0.02519	0.3397±0.02595	3.516	0.0009
T2-mapping value (ms), mean±SD	67.53±4.591	79.30±8.797	5.749	<0.0001

*, Fisher's test.

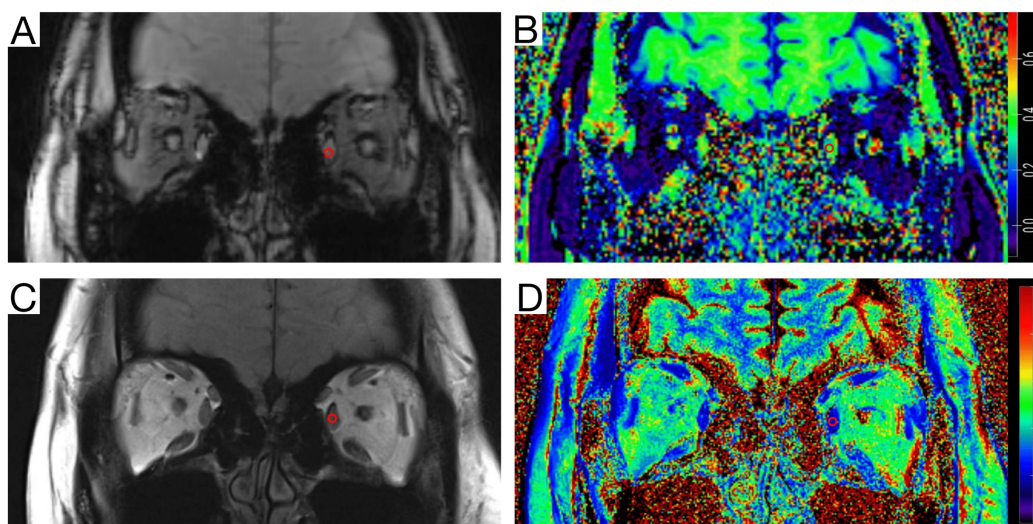


Figure 1. Measurement diagram of the magnetization transfer ratio (MTR) and T2-mapping value. A circular region of interest (ROI) (area of 5-10 mm²) was delineated on the coronal orbital T2 anatomical mapping image with the largest cross-sectional area of the ocular muscles of myasthenia gravis (MG) patients and healthy volunteers. The ROI was then copied to the T2-mapping image, and the corresponding T2 signal values were recorded. On the same level of the Magnetization transfer off (MT-off) map, the same ROI (area of 5-10 mm²) was delineated, the ROI was copied to the MTR image, and the corresponding MTR value was recorded. **A**, MT-off image. **B**, MTR image. **C**, T2-anatomical mapping image. **D**, T2-mapping image.

MG patients showed significantly higher means of MTR and T2-mapping values in the extraocular muscles compared with healthy controls

The mean MTR value of the extraocular muscles was significantly higher in MG patients compared with healthy controls (Table 2). Similarly, the mean T2-mapping value in MG patients was significantly higher than healthy controls (Table 2).

Table 2. Comparison of the mean magnetization transfer ratio (MTR) and T2-mapping values, and clinical characteristics, between myasthenia gravis (MG) patients with ophthalmoparesis (MG-O) and without ophthalmoparesis (MG-N)

	MG-O (n=13)	MG-N (n=19)	T or Z value	P value
MTR, mean	0.3285±0.02533	0.3473±0.02408	2.131	0.0414
T2 mapping value, mean	83.12±8.732	76.69±8.043	2.147	0.0400
Age	49.54±17.17 (18-77)	41.84±18.51 (16-71)	1.189	0.2438
Sex (male:female)	7:6	1:18		
Antibody types, AChR: MuSK, n	12:1	16:3		
Duration, months, median (IQR)	32.00 (7.55, 79.84)	25.10 (11.77, 61.30)		0.5962
Drug therapy, n				
Pyridostigmine	13	19		
Corticosteroid	11	17		
Immunosuppressants	9	13		
Highest dose of corticosteroid, as prednisone, milligram, mean±SD	25.39±21.55	19.21±15.66	0.9402	0.3546
Kinds of immunosuppressant used, n				
One	5	9		
More than one	4	4		
MG subtypes, n				
OMG	1	0		
Early-onset GMG	3	12		
Late-onset GMG	8	6		
MG with thymoma	1	1		
MGFA type, n				
I	2	0		
II	3	7		
III	6	11		
IV	2	1		
V	0	0		
Thymectomy status, n				
Without thymectomy	7	17		
Thymectomy	6	2		
Neurophysiology, n				
RNS+	6	6		
RNS- and SFEMG+	0	1		
All negative	0	0		
Unknown	7	12		

MG-N, MG patients without ophthalmoparesis; MG-O, MG patients with ophthalmoparesis; SD, standard deviation; AChR, acetylcholine receptor; MuSK, muscle-specific kinase; IQR, interquartile range; OMG, ocular MG; GMG, generalized MG; MGFA, myasthenia gravis foundation of America; RNS, repetitive nerve stimulation; SFEMG, single fiber electromyogram.

Patients with ophthalmoparesis had a significantly lower mean MTR, but a higher mean T2-mapping value, than patients without ophthalmoparesis

There is currently no clinical standard for assessing the severity of extraocular muscle involvement in MG patients. In the present study, we classified patients into those with (MG-O) and without (MG-N) ophthalmoparesis based on the extent of eye movement limitation. Patients with ophthalmoparesis are considered to have more severe extraocular muscle involvement. Of the 32 patients in the present study, 13 had ophthalmoparesis (MG-O) and 19 did not (MG-N). From the healthy controls, MG-N patients, and MG-O patients, the MG-N group had the highest average MTR (Fig. 2a), while the MG-O group had the highest average T2-mapping value (Fig. 2b).

Combined MTR and T2-mapping values significantly differentiate between normal and MG-affected extraocular muscles

In Fig. 3A, ROC curve analysis showed that using an MTR of 0.3396 as a threshold to predict whether MG patients had extraocular muscle involvement resulted in an AUC (95% confidence interval (CI)) of 0.7443 (0.6138-0.8748; $p = 0.0025$), with a sensitivity of 53.13%, specificity of 95.45%, and accuracy of 68.52%. Using a T2-mapping value of 72.65 ms as a threshold, the AUC (95% CI) was 0.8835 (0.7954-0.9716; $p < 0.001$), with a sensitivity of 78.13%, specificity of 86.36%, and accuracy of 81.48%. There was no difference in AUC between the MTR and the T2-mapping value for predicting MG extraocular muscle involvement ($Z = 1.732$, $p = 0.0832$). The combined use of MTR and the T2-mapping value yielded an AUC (95% CI) of 0.9261 (0.8600-0.9923; $p < 0.001$), with a sensitivity of 84.38%, specificity of 90.91%, and accuracy of 87.04%. The combined predictive power of the MTR and the T2-mapping values was superior to MTR alone ($Z = 2.436$, $p = 0.0149$), but not significantly different from the T2-mapping value alone ($Z = 0.7579$, $p = 0.4485$).

Combined MTR and T2-mapping values can differentiate the severity of extraocular muscle involvement in MG patients

In Fig. 3B, ROC curve analysis showed that using an MTR of 0.3330 as a threshold to predict severe extraocular muscle involvement in MG patients resulted in an AUC (95% CI) of 0.7206 (0.5341-0.9072; $p = 0.0365$), with a sensitivity of 73.68%, specificity of 69.23%, and accuracy of 71.88%. Using a T2-mapping value of 81.45 ms as a threshold, the AUC (95% CI)

was 0.7126 (0.5181-0.9070; $p = 0.0440$), with a sensitivity of 78.95%, specificity of 69.23%, and accuracy of 71.88%. The difference in AUC between the MTR and the T2-mapping value for predicting severe extraocular muscle involvement in MG patients was not significant ($Z = 0.0582$, $p = 0.9536$). The combined use of MTR and the T2-mapping value yielded an AUC (95% CI) of 0.7895 (0.6338-0.9451; $p = 0.0061$), with a sensitivity of 63.16%, specificity of 84.62%, and accuracy of 71.88%. The combined predictive power of the MTR and the T2-mapping values was similar to MTR alone ($Z = 0.5557$, $p = 0.5784$) and the T2-mapping value alone ($Z = 0.6051$, $p = 0.5451$).

Discussion

We previously described the utility of three-dimension time-of-flight magnetic resonance angiography sequences for measuring the extraocular muscle volume in MG patients. In the present study [24], we further used MTI and T2-mapping sequences and found that the MTR and the T2-mapping value of the extraocular muscles were significantly higher in MG patients compared with age-matched healthy controls [25]. However, within the MG patient group, patients with ophthalmoparesis had lower MTR values but higher T2-mapping values compared with those without ophthalmoparesis.

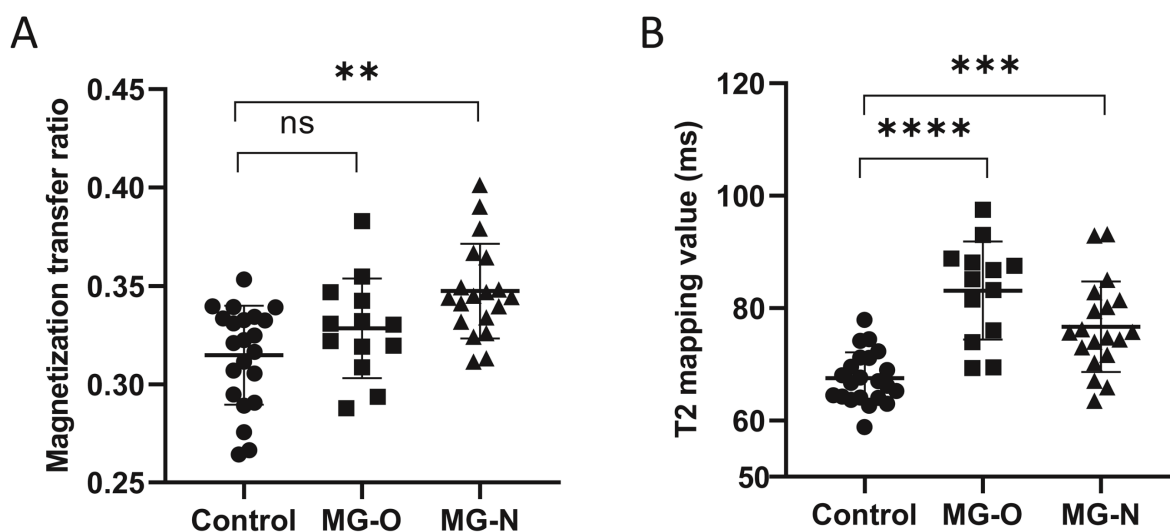


Figure 2. Comparison of the magnetization transfer ratio (MTR) (A) and the T2-mapping values (B) in healthy controls, myasthenia gravis (MG) patients with ophthalmoparesis (MG-O group), and MG patients without ophthalmoparesis (MG-N group). ns, not significant. **, $p < 0.01$; ***, $p < 0.001$; ****, $p < 0.0001$.

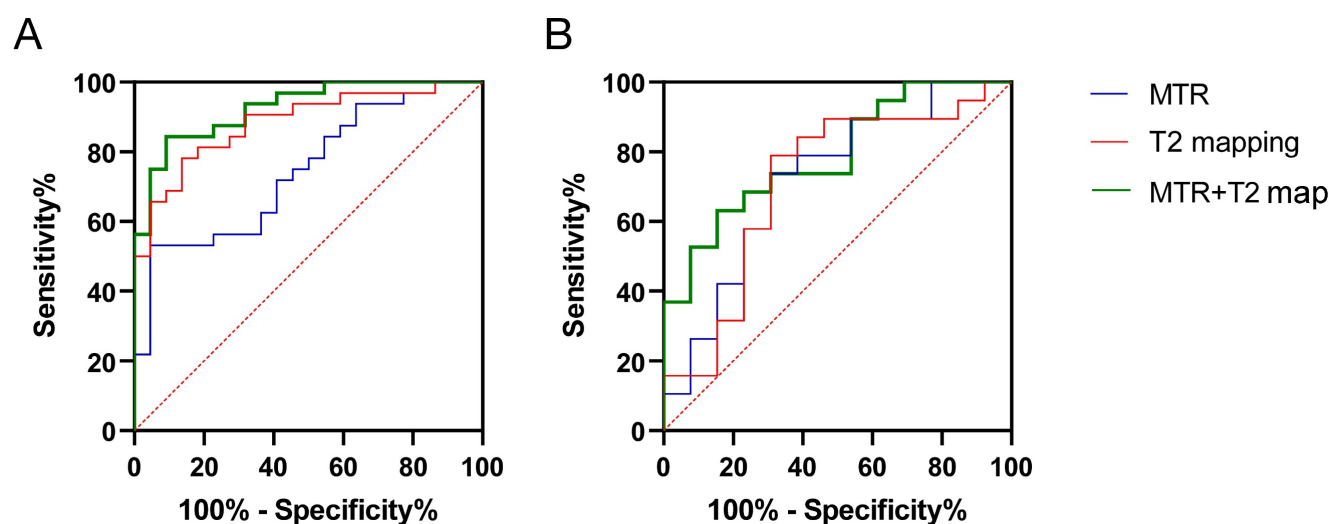


Figure 3. Receiver operating characteristic (ROC) curve analysis of MRI quantitative parameters (magnetization transfer ratio [MTR] and the T2-mapping value [ms]) for diagnosing and differentiating the severity of inflammation in the extraocular muscles of myasthenia gravis (MG) patients. (A) Diagnostic efficacy of combined MRI quantitative parameters (MTR and the T2-mapping value) in the extraocular muscles of MG patients. (B) Efficacy of combined MRI quantitative parameters (MTR and the T2-mapping value) in differentiating the severity of inflammation in the extraocular muscles of MG patients with ophthalmoparesis (MG-O) and without ophthalmoparesis (MG-N) (MG-O vs. MG-N groups). Blue line, MTR. Red line, T2-mapping value. Green line, combined MTR + T2-mapping value.

Chronic inflammation often leads to fibrosis in muscle tissue, which results in an increase in connective tissue and large molecules [26], thereby elevating the MTR of muscle tissue [27, 28]. Thus, the MTR reflects the degree of tissue fibrosis. The inflammatory response caused by MG autoantibodies can primarily affect the extraocular muscles, which leads to related symptoms. Because MG is not curable and patients always have high levels of autoantibodies, their extraocular muscle tissues may remain in an extended state of chronic inflammation [29, 30]. In turn, this may cause significant fibrosis, as reflected by an elevated MTR, in the extraocular muscles of MG patients, as shown in the present study [31].

T2-mapping values reflect the water content in muscle tissue [32, 33]. In GO, T2-mapping values are often used to quantify the degree of inflammatory edema in the extraocular muscles during the active phase of the disease. Therefore, increased T2-mapping values could indicate acute inflammation in muscle tissue. Clinically, MG patients often experience relapses, and muscle weakness can signify worsening or recurrence of the condition [34]. During the recurrence times, acute inflammation is occurring in the muscle tissue, which causes significantly higher T2-mapping values, especially in patients with ophthalmoparesis.

In the present study, ROC curve analysis of combined MTR and T2-mapping values showed significant differences between the extraocular muscles of MG patients and healthy controls, and using both measures together could distinguish between affected and normal extraocular muscles. However, in clinical practice, using MRI parameters of the extraocular muscles to diagnose MG may not be necessary, and we plan to explore new applications for these MRI sequences. For example, in studies of extraocular muscles in GO, combining MTR and T2-mapping values was helpful for assessing inflammatory activity [35]. In MG patients, relying solely on clinical symptoms of extraocular muscle involvement to determine the degree of inflammation has notable limitations [36]. The sensitivity of patients to extraocular muscle symptoms may vary. Some patients do not notice a significant impact on their lives from extraocular muscle symptoms, particularly if they lack diplopia or severe ptosis [37], and therefore may not prioritize these symptoms during medical visits [38]. Additionally, neurologists may not always focus on extraocular muscle symptoms or link them to chronic inflammation. Given the relatively objective nature of MRI results, MRI may be a valuable complementary tool for evaluating inflammation in extraocular muscles.

Note that we used the range of eye movement as a clinical standard for assessing extraocular muscle involvement, with limited eye movement (i.e., ophthalmoparesis) considered an indicator of severe inflammation [39]. Based on this standard, ROC curve analysis of combined MTR and T2-mapping values could differentiate between clinically different severities of extraocular muscle involvement [40]. However, we observed some inconsistencies when we used the mean MTR and T2-mapping values to differentiate the degree of inflammatory response in the extraocular muscles of MG patients. For instance, MTR values were lower in patients with severe inflammation and ophthalmoparesis compared with healthy controls, despite the overall higher MTR values in MG patients [41]. This may be caused by the significant increase in water content in the extraocular muscles during acute inflammation (i.e., higher T2-mapping values), which could lower the MTR values, as per the principles of MTR measurement [42-44].

We previously reported that the extraocular muscle volume in MG-O patients was lower than that in MG-N patients, and that this volume was negatively correlated with disease duration in MG-N patients [45, 46]. These findings indirectly suggest that MG patients with ophthalmoparesis may be in a chronic inflammatory state, which leads to muscle fibrosis. In the present study, we further examined the relationship between MTR values and disease duration. To exclude the effects of edema from acute inflammation, we examined the correlations between MTR values and disease duration in MG-N patients. However, we found no significant correlation, which suggests that with long-term appropriate treatment, patients may effectively control muscle tissue inflammation and avoid fibrosis [45, 47].

The significance of this study lies in its clinical application—a lower MTR and a higher T2-mapping value in an MG patient indicates severe inflammation in the extraocular muscles. Regardless of ophthalmoparesis, prompt and aggressive treatment may be appropriate [48]. This reflects the potential clinical significance of these MRI measurements. Moreover, because corticosteroids and immunosuppressants often have slow effects in treating MG, treatment adjustments may be delayed, which leads to suboptimal outcomes and increased side effects from prolonged medication use. MRI analysis of the extraocular muscles in MG patients can contribute to the early assessment of whether treatment is effectively controlling inflammation. Nevertheless, this study has several limitations, which include a small sample size, lack of more objective clinical standards for assessing extraocular muscle

involvement, and the absence of detailed clinical evaluation standards that could allow different eyes of the same patient to be studied separately (as previously reported in GO [49]), which would make it easier to collect sufficient clinical samples and conduct more precise studies.

In conclusion, analysis of the extraocular muscles in MG patients using special MRI sequences identified potential markers for assessing the degree of inflammatory extent in these muscles. These findings provide a reference for guiding precise treatment.

Abbreviations

EOM: extraocular muscle; MRI: magnetic resonance imaging; MTI: magnetization transfer imaging; MTR: magnetization transfer ratio; ROC: receiver operating characteristic; ROI: region of interest; GO: Graves' ophthalmopathy; MT: magnetization transfer; MG: myasthenia gravis; AChEI: acetylcholinesterase inhibitors; MuSK: muscle-specific kinase; MG-O: myasthenia gravis patients with ophthalmoparesis; MG-N: myasthenia gravis patients without ophthalmoparesis; SD: standard deviation; IQR: interquartile range; CI: confidence interval; AChR: acetylcholine receptor; MuSK: muscle-specific kinase; IQR: interquartile range; OMG: ocular MG; GMG: generalized MG; MGFA: myasthenia gravis foundation of America; RNS: repetitive nerve stimulation; SFEMG: single fiber electromyogram.

Acknowledgements

We acknowledge the National Natural Science Foundation of China, Guangdong Provincial Key Laboratory of Diagnosis and Treatment of Major Neurological Diseases (2020B1212060017), Guangdong Provincial Clinical Research Center for Neurological Diseases (2020B111170002), Southern China International Joint Research Center for Early Intervention and Functional Rehabilitation of Neurological Diseases (2015B050501003 and 2020A0505020004), Guangdong Provincial Engineering Center for Major Neurological Disease Treatment, Guangdong Provincial Translational Medicine Innovation Platform for Diagnosis and Treatment of Major Neurological Disease, Guangzhou Clinical Research and Translational Center for Major Neurological Diseases (201604020010).

Author contributions

Q.Z., X.Z. and P.C. contributed to the manuscript writing – original draft and submission. X.Z., M.W., Y.L., and Q.Z. contributed to data collection, entry, processing and statistical analysis. P.C. contributed to

the clinical information collection and patient's follow-up. Z.Y. contributed to review and edit the manuscript. P.C. and W.L., the corresponding authors, conceptualized, initiated, and oversaw the entire project, designed and supervised the project conduction, and review the manuscript. W.L. diagnosed and treated most cases. All authors reviewed drafts of the manuscript and approved the final submitted manuscript. All authors attest to the integrity of the data.

Ethics approval

Ethics approval for this study was obtained from the First Affiliated Hospital of Sun Yat-sen University research ethics committee (No. 2022-666).

Consent to participate

Informed consent was obtained from all individual participants included in the study.

Consent to publish

The authors affirm that human research participants provided informed consent for publication of the images in Fig. 1.

Competing Interests

The authors have declared that no competing interest exists.

References

1. Drachman DB. Myasthenia Gravis. *Semin Neurol.* 2016; 36: 419-24.
2. Gilhus NE. Myasthenia Gravis. *N Engl J Med.* 2016; 375: 2570-81.
3. Europa TA, Nel M, Heckmann JM. Myasthenic ophthalmoparesis: Time To resolution after initiating immune therapies. *Muscle Nerve.* 2018; 58: 542-9.
4. Kaminski HJ, Li Z, Richmonds C, Lin F, Medof ME. Complement regulators in extraocular muscle and experimental autoimmune myasthenia gravis. *Exp Neurol.* 2004; 189: 333-42.
5. Dou L, Lu E, Tian D, Li F, Deng L, Zhang Y. Adrenomedullin induces cisplatin chemoresistance in ovarian cancer through reprogramming of glucose metabolism. *J Transl Int Med.* 2023; 11: 169-77.
6. Benatar M, McDermott MP, Sanders DB, Wolfe GI, Barohn RJ, Nowak RJ, et al. Efficacy of prednisone for the treatment of ocular myasthenia (EPITOME): A randomized, controlled trial. *Muscle Nerve.* 2016; 53: 363-9.
7. Deng Y, Wang H, Guo X, Jiang S, Cai J. Long-term blood pressure outcomes of laparoscopic adrenalectomy in rHTN patients. *J Transl Int Med.* 2023; 11: 275-81.
8. Sollmann N, Weidlich D, Klupp E, Cervantes B, Ganter C, Zimmer C, et al. T2 mapping of the distal sciatic nerve in healthy subjects and patients suffering from lumbar disc herniation with nerve compression. *Magma.* 2020; 33: 713-24.
9. Jiang M, Song X, Zhang H, Tao X, Yang G, Wang Y, et al. The combination of T2-mapping value of lacrimal gland and clinical indicators can improve the stage prediction of Graves' ophthalmopathy compared to clinical activity scores. *Endocrine.* 2022; 78: 321-8.
10. Trattig S, Millington SA, Szomolanyi P, Marlovits S. MR imaging of osteochondral grafts and autologous chondrocyte implantation. *Eur Radiol.* 2007; 17: 103-18.
11. Meng J, Huang S, Sun C, Zhang ZW, Mao R, Yang YH, et al. Comparison of Three Magnetization Transfer Ratio Parameters for Assessment of Intestinal Fibrosis in Patients with Crohn's Disease. *Korean J Radiol.* 2020; 21: 290-7.
12. MacDonald ME, Pike GB. MRI of healthy brain aging: A review. *NMR Biomed.* 2021; 34: e4564.
13. Chen X, Wang M, Yu K, Xu S, Qiu P, Lyu Z, et al. Chronic stress-induced immune dysregulation in breast cancer: Implications of psychosocial factors. *J Transl Int Med.* 2023; 11: 226-33.
14. Schawkat K, Eshmunov D, Lenggenger D, Endhardt K, Vrugt B, Boss A, et al. Preoperative Evaluation of Pancreatic Fibrosis and Lipomatosis: Correlation of Magnetic Resonance Findings With Histology Using

- Magnetization Transfer Imaging and Multigradient Echo Magnetic Resonance Imaging. *Invest Radiol.* 2018; 53: 720-7.
15. Li XH, Mao R, Huang SY, Sun CH, Cao QH, Fang ZN, et al. Characterization of Degree of Intestinal Fibrosis in Patients with Crohn Disease by Using Magnetization Transfer MR Imaging. *Radiology.* 2018; 287: 494-503.
 16. Martens MH, Lambregts DM, Papanikolaou N, Heijnen LA, Riedl RG, zur Hausen A, et al. Magnetization transfer ratio: a potential biomarker for the assessment of postirradiation fibrosis in patients with rectal cancer. *Invest Radiol.* 2014; 49: 29-34.
 17. Chang EY, Suprana A, Tang Q, Cheng X, Fu E, Orozco E, et al. Rotator cuff muscle fibrosis can be assessed using ultrashort echo time magnetization transfer MRI with fat suppression. *NMR Biomed.* 2024; 37: e5058.
 18. López K, Neji R, Bustin A, Rashid I, Hajhosseiny R, Malik SJ, et al. Quantitative magnetization transfer imaging for non-contrast enhanced detection of myocardial fibrosis. *Magn Reson Med.* 2021; 85: 2069-83.
 19. Deng M, Wang M, Zhang Q, Jiang B, Yan L, Bian Y, et al. Point-of-care ultrasound-guided submucosal paclitaxel injection in tracheal stenosis model. *J Transl Int Med.* 2023; 11: 70-80.
 20. Chen P, Zhou Q, Zhao X, Chen Y, Lin Z, Wang M, et al. Extraocular muscle volume on time-of-flight magnetic resonance angiography in patients with myasthenia gravis. *Muscle Nerve.* 2024; 70: 379-86.
 21. Cakir MU, Yavuz-Aksu B, Aksu U. Hypervolemia suppresses dilutional anaemic injury in a rat model of haemodilution. *J Transl Int Med.* 2023; 11: 393-400.
 22. Kollmer J, Kessler T, Sam G, Hayes JM, Lentz SI, Heiland S, et al. Magnetization transfer ratio: a quantitative imaging biomarker for 5q spinal muscular atrophy. *Eur J Neurol.* 2021; 28: 331-40.
 23. DeLong ER, DeLong DM, Clarke-Pearson DL. Comparing the areas under two or more correlated receiver operating characteristic curves: a nonparametric approach. *Biometrics.* 1988; 44: 837-45.
 24. Jiang L, Chen T, Xiong L, Xu JH, Gong AY, Dai B, et al. Knockdown of m6A methyltransferase METTL3 in gastric cancer cells results in suppression of cell proliferation. *Oncol Lett.* 2020; 20: 2191-8.
 25. E IR, Bakarozzi M, Dimas I, Galanis K, Lygoura V, N KG, et al. Total and individual PBC-40 scores are reliable for the assessment of health-related quality of life in Greek patients with primary biliary cholangitis. *J Transl Int Med.* 2023; 11: 246-54.
 26. Alameddine HS, Morgan JE. Matrix Metalloproteinases and Tissue Inhibitor of Metalloproteinases in Inflammation and Fibrosis of Skeletal Muscles. *J Neuromuscul Dis.* 2016; 3: 455-73.
 27. Li K, Dortch RD, Welch EB, Bryant ND, Buck AK, Towse TF, et al. Multi-parametric MRI characterization of healthy human thigh muscles at 3.0 T - relaxation, magnetization transfer, fat/water, and diffusion tensor imaging. *NMR Biomed.* 2014; 27: 1070-84.
 28. Bryant ND, Li K, Does MD, Barnes S, Gochberg DF, Yankeelov TE, et al. Multi-parametric MRI characterization of inflammation in murine skeletal muscle. *NMR Biomed.* 2014; 27: 716-25.
 29. Li J, Allende A, Martin F, Fraser CL. Histopathological changes of fibrosis in human extra-ocular muscle caused by botulinum toxin A. *J aapos.* 2016; 20: 544-6.
 30. He Q, Li J. The evolution of folate supplementation - from one size for all to personalized, precision, poly-paths. *J Transl Int Med.* 2023; 11: 128-37.
 31. Huang Z, Yu P, Tang J. Characterization of Triple-Negative Breast Cancer MDA-MB-231 Cell Spheroid Model. *Onco Targets Ther.* 2020; 13: 5395-405.
 32. O'Brien AT, Gil KE, Varghese J, Simonetti OP, Zareba KM. T2 mapping in myocardial disease: a comprehensive review. *J Cardiovasc Magn Reson.* 2022; 24: 33.
 33. Hyug Choi J, Sook Jun M, Yong Jeon J, Kim HS, Kyung Kim Y, Ho Jeon C, et al. Global lineage evolution pattern of sars-cov-2 in Africa, America, Europe, and Asia: A comparative analysis of variant clusters and their relevance across continents. *J Transl Int Med.* 2023; 11: 410-22.
 34. Gao WL, Li XH, Dun XP, Jing XK, Yang K, Li YK. Grape Seed Proanthocyanidin Extract Ameliorates Streptozotocin-induced Cognitive and Synaptic Plasticity Deficits by Inhibiting Oxidative Stress and Preserving AKT and ERK Activities. *Curr Med Sci.* 2020; 40: 434-43.
 35. Li Y, Yao Z, Li Y, Yang Z, Li M, Chen Z, et al. Prognostic value of serum ammonia in critical patients with non-hepatic disease: A prospective, observational, multicenter study. *J Transl Int Med.* 2023; 11: 401-9.
 36. Ding L, Lu S, Zhou Y, Lyu D, Ouyang C, Ma Z, et al. The 3' Untranslated Region Protects the Heart from Angiotensin II-Induced Cardiac Dysfunction via AGGF1 Expression. *Mol Ther.* 2020; 28: 1119-32.
 37. Lu Y, Lin Z, Wen L, Gao W, Pan L, Li X, et al. The Adaptation and Acceptance of Defocus Incorporated Multiple Segment Lens for Chinese Children. *Am J Ophthalmol.* 2020; 211: 207-16.
 38. Liu N, Li D, Liu D, Liu Y, Lei J. FOSL2 participates in renal fibrosis via SGK1-mediated epithelial-mesenchymal transition of proximal tubular epithelial cells. *J Transl Int Med.* 2023; 11: 294-308.
 39. Cuny H, Bozon K, Kirk RB, Sheng DZ, Bröer S, Dunwoodie SL. Maternal heterozygosity of Slc6a19 causes metabolic perturbation and congenital NAD deficiency disorder in mice. *Dis Model Mech.* 2023; 16: dmm049647.
 40. Peng Y, Wang Y, Zhou C, Mei W, Zeng C. PI3K/Akt/mTOR Pathway and Its Role in Cancer Therapeutics: Are We Making Headway? *Front Oncol.* 2022; 12: 819128.
 41. Chen L, Zhan CZ, Wang T, You H, Yao R. Curcumin Inhibits the Proliferation, Migration, Invasion, and Apoptosis of Diffuse Large B-Cell Lymphoma Cell Line by Regulating MiR-21/VHL Axis. *Yonsei Med J.* 2020; 61: 20-9.
 42. Duchesne E, Dufresne SS, Dumont NA. Impact of Inflammation and Anti-inflammatory Modalities on Skeletal Muscle Healing: From Fundamental Research to the Clinic. *Phys Ther.* 2017; 97: 807-17.
 43. Pazahr S, Blume I, Frei P, Chuck N, Nanz D, Rogler G, et al. Magnetization transfer for the assessment of bowel fibrosis in patients with Crohn's disease: initial experience. *Magma.* 2013; 26: 291-301.
 44. Shao Y, Zhao T, Zhang W, He J, Lu F, Cai Y, et al. Presence of the apolipoprotein E-ε4 allele is associated with an increased risk of sepsis progression. *Sci Rep.* 2020; 10: 15735.
 45. Chen L, Tian Q, Shi Z, Qiu Y, Lu Q, Liu C. Melatonin Alleviates Cardiac Function in Sepsis-Induced Myocarditis via Maintenance of Mitochondrial Function. *Front Nutr.* 2021; 8: 754235.
 46. Wen L, Cao Y, Cheng Q, Li X, Pan L, Li L, et al. Objectively measured near work, outdoor exposure and myopia in children. *Br J Ophthalmol.* 2020; 104: 1542-7.
 47. Yu W, Qin X, Zhang Y, Qiu P, Wang L, Zha W, et al. Curcumin suppresses doxorubicin-induced cardiomyocyte pyroptosis via a PI3K/Akt/mTOR-dependent manner. *Cardiovasc Diagn Ther.* 2020; 10: 752-69.
 48. Menon D, Alharbi M, Katzberg HD, Bril V, Mendoza MG, Barnett-Tapia C. Effect of Immunosuppression in Risk of Developing Generalized Symptoms in Ocular Myasthenia Gravis: A Retrospective Cohort Study. *Neurology.* 2024; 103: e209722.
 49. Zhang L, Jiang B, Zhu N, Tao M, Jun Y, Chen X, et al. Mitotic checkpoint kinase Mps1/TTK predicts prognosis of colon cancer patients and regulates tumor proliferation and differentiation via PKCα/ERK1/2 and PI3K/Akt pathway. *Med Oncol.* 2019; 37: 5.